Multiphoton ionization and photoelectron spectroscopy of formaldehyde via its 3*p* Rydberg states

Jianbo Liu, Ho-Tae Kim, and Scott L. Anderson
Department of Chemistry, University of Utah, 315 S. 1400 E. RM Dock, Salt Lake City, Utah 84112-0850

(Received 18 December 2000; accepted 20 March 2001)

The resonance-enhanced multiphoton ionization (REMPI) spectrum of formaldehyde, two photon resonant in the region of the $^1A_2(3p_x)$, $^1A_1(3p_y)$, and $^1B_2(3p_z)$ states, is reported. The $^1A_2(3p_x)$ state spectrum is dominated by the ν_3' (CH_2 scissors), ν_4' (CH_2 out-of-plane bending), ν_5' (CH_2 asymmetric stretching), and ν_6' (CH_2 rock) modes, with weaker bands observed for excitation of the ν_2' (CO stretching) mode. Vibrational analysis of the spectrum provides many new frequencies for the $^1A_2(3p_x)$ state, not resolved or accessible in single photon spectroscopic measurements. Photoelectron spectroscopy is used to probe the nature of the vibronic levels associated with the $^1A_2(3p_x)$ intermediate state, to measure vibrational frequencies of the resulting cations, and to identify useful routes for preparing vibrational state-selected H_2CO^+. It is found that $H_2CO[^1A_2(3p_x)]$ is a well-behaved Rydberg state, generating cations in the same vibrational level that was populated in the intermediate. Cations with mode-selective excitation of up to 0.62 eV can be produced. *Ab initio* calculations are used to help assign the cation vibrations. In contrast to the well-behaved $^1A_2(3p_x)$ state, the $^1A_1(3p_y)$ and $^1B_2(3p_z)$ states are strongly mixed with each other and with valence states. © *2001 American Institute of Physics.* [DOI: 10.1063/1.1370943]

I. INTRODUCTION

Vibrational state selection provides a powerful tool for probing reaction mechanisms for small polyatomic cation systems.[1–12] By combining mode-selective reactant preparation with measurement of product recoil velocity distributions, quite a complete picture of the reaction dynamics can be extracted. A major limiting factor in such studies is discovering ionization routes by which cations can be produced with controllable excitation in particular vibrational modes. Resonance-enhanced multiphoton ionization (REMPI) can be a simple and effective state-selective ionization tool, but only for molecules with the proper spectroscopic properties.[13] In REMPI vibrational state selection, the neutral precursor molecule is pumped with one or more photons to a particular vibrational level of an intermediate electronic state, then is ionized by a single additional photon. The vibrational state distribution of the resulting ions depends on the transition probabilities coupling the intermediate level with all energetically accessible states of the ion plus electron. In the case where the intermediate is a Rydberg state with little perturbation from valence states, the vibrational wave functions of the Rydberg molecule and the resulting ion are nearly orthogonal, and the Franck–Condon factors for ionization of the Rydberg state are diagonal, i.e., the ion is formed predominantly in the same vibrational level that was selected in the intermediate. The actual cation vibrational distribution is revealed by the photoelectron spectrum measured following ionization through the intermediate state, and the spectrum also gives insight into the nature of the intermediate state.

This paper reports a REMPI and photoelectron spectroscopy study of formaldehyde (H_2CO), with the goal of finding routes for preparing state-selected H_2CO^+. In addition to finding excellent state selection routes, the results shed some new light on the 3*p* Rydberg states of this well-studied molecule. The literature concerning the spectroscopy of H_2CO is sizable, including studies of emission,[14] absorption,[14–25] electric dichroism spectroscopy,[26] electron-impact spectroscopy,[27,28] multiphoton ionization,[29–31] photoelectron spectroscopy,[32–35] ZEKE-PFI,[36] and photoionization spectroscopy.[19,37,38] These studies have revealed much concerning the geometries, transition energies, and rovibronic energy levels for the ground and excited states for both neutral and ionic formaldehyde. Parallel to these experiments, theoretical progress has been made in providing reliable predictions for the interpretation of spectroscopic observations.[39–57] Much of this work has focused on the valence states of H_2CO, and the Rydberg states have not received as much attention. The absence of 2+1 REMPI studies is particularly surprising, considering that two photon spectroscopy can probe states not seen in single photon studies.[48,58] Certainly, the next higher homologue, acetaldehyde, has been the subject of several 2+1 REMPI studies.[59–62]

To our knowledge, the only REMPI studies probing the energy range of the 3*p* Rydberg states were with 3+1 (Ref. 29) and 1+2+1 (Ref. 30) REMPI schemes. These REMPI studies covered only a narrow photon energy range, mainly probing the origin bands and a few low energy vibrations of the $^1A_2(3p_x)$, $^1A_1(3p_y)$, and $^1B_2(3p_z)$ states. We have obtained the 2+1 REMPI spectrum of H_2CO in the two-photon energy range from 64 000 to 73 500 cm^{-1}, probing transitions to the $^1A_2(3p_x)$, $^1A_1(3p_y)$, and $^1B_2(3p_z)$ Rydberg states. As expected, many vibronic bands identified in the present experiment were not resolved or accessible in previous absorption and REMPI measurements. Furthermore,

photoelectron spectroscopy has been used to probe the nature of the vibronic levels associated with the $^1A_2(3p_x)$ Rydberg state, and many useful routes for preparation of vibrationally state-selected H_2CO^+ have been identified. To provide a reliable interpretation of the PES results, we also performed *ab initio* calculations of H_2CO^+ at various levels of theory. The geometry of the H_2CO^+ ion is determined to be planar, and a low vibrational frequency in cation, assigned in the previous He I photoelectron spectra as the ν_4^+ (out-of-plane bending) mode,[33,34] is reassigned as the ν_6^+ (CH_2 rock) mode, as suggested by Bruna *et al.*[57] A somewhat higher frequency mode, not seen in the He I PES, is assigned as ν_4^+. Several other previously unobserved vibrational bands of the cation are identified.

II. EXPERIMENT

The experiments were performed on a homemade photoelectron/photoion time-of-flight spectrometer.[62] The laser beam was generated by a Continuum Nd:YAG-pumped dye laser (NY82S/ND6000) using a total of five dyes (exciton rhodamine 640, 610, 610/590, 590, and fluorescein 548). The dye laser output was frequency-doubled by an Inrad Autotracker, producing average UV pulse energies of 5–7 mJ. The laser was focused with a 15 cm focal length lens into the center of the ionization region.

Monomeric H_2CO gas was obtained by heating a mixture of solid paraformaldehyde (Aldrich 95%) and anhydrous $MgSO_4$ (Merck), held in a stainless steel tube connected directly to a pulsed molecular beam valve. The tube and pulsed nozzle were heated to 60 °C causing the paraformaldehyde to liberate monomeric H_2CO and water.[63] The water was absorbed by the $MgSO_4$, and the monomeric H_2CO was swept into the pulsed valve by a flow of helium at ~1 atm. The vapor pressure of H_2CO is estimated to be around 0.047 atm at 60 °C,[64] hence the concentration of H_2CO in the molecular beam was around 5%. The mixed gas was then introduced into the photoionization region as a pulsed, skimmed molecular beam at 10 Hz. Because H_2CO readily repolymerizes in the presence of water,[65] the entire gas line was baked at 400 K before use, the distance from the generation of H_2CO to the supersonic expansion was minimized, and the helium was passed through a molecular sieve trap maintained at 77 K. This procedure greatly reduced the repolymerization of H_2CO; no dimer, trimer or fragments attributable to them could be detected in the mass spectra.

A. REMPI spectra

Two types of 2+1 REMPI spectra were recorded. The first is a wavelength scan of the total photoelectrons, in which the photoelectrons were produced in an ionization region formed by a pair of planar grids separated by ~1 cm. The upper grid was grounded and the lower grid was set at a negative dc potential (−5 V) to maximize collection efficiency of the electrons. After acceleration the electrons enter a 0.75 m-long magnetically shielded, field-free flight tube ending in a multichannel plate.

We also recorded spectra while monitoring the parent ion signal. These experiments were carried out in the same instrument by adding a third grid to the ionization region, converting the photoelectron spectrometer to a time-of-flight (TOF) mass spectrometer. This arrangement was also used to get the REMPI mass spectra of formaldehyde at fixed wavelengths. Both ion and electron signals were amplified, collected by a Tektronix 500M digital oscilloscope, and transferred to a PC for analysis. No attempt was made to normalize the spectra for variations in laser intensity (±20%).

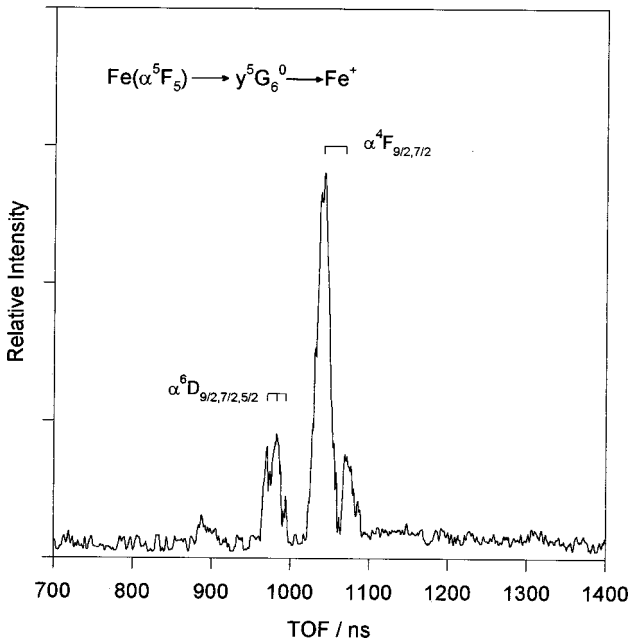

FIG. 1. Typical 1+1 MPI photoelectron calibration spectrum of atomic iron following photolysis of $Fe(CO)_5$.

B. Time-of-flight photoelectron spectra

Photoelectron kinetic energy spectra were also measured by TOF, using the same instrument. The only difference was that no acceleration fields were used, so as to not degrade the electron energy resolution. The collection efficiency ($\sim 10^{-4}$) is determined by the solid angle subtended by the detector. For each photoelectron spectrum (PES), the laser intensity was kept as low as possible to avoid peak broadening due to space charge effects, while keeping the signal well above the noise. Spectra were corrected for background by subtracting TOF spectra obtained with the molecular beam on and off, each signal averaged for 10 000 laser shots.

The energy calibration of the TOF PES was carried out by using 1+1 REMPI PES of the iron atom as described by Anderson *et al.*[66] Fe atoms were produced by photolysis of $Fe(CO)_5$ (Aldrich), and REMPI transitions of Fe from $Fe(CO)_5$ have been previously assigned by Whetten *et al.*[67] The PES of Fe^+ ionized via three different REMPI transitions ($\alpha^5F_5 \rightarrow y^5G_6^0$ at 278.901 nm, $\alpha^5F_4 \rightarrow y^5G_5^0$ at 281.427 nm and $\alpha^5F_3 \rightarrow y^5G_4^0$ at 283.337 nm) were obtained, and the assignment of the PES peaks is straightforward as exemplified for the $\alpha^5F_5 \rightarrow y^5G_6^0 \rightarrow Fe^+$ transition shown in Fig. 1. The photoelectron energies of these peaks were calculated from energy levels of Fe and Fe^+ given by Sugar and Corliss.[68] The result is a set of 14 accurately known PES

TABLE I. Experimental and calculated frequencies of $H_2CO[\tilde{X}\,^1A_1]$ and $H_2CO^+[\tilde{X}\,^2B_2]$.[a]

	$H_2CO[\tilde{X}\,^1A_1]$		$H_2CO^+[\tilde{X}\,^2B_2]$		
			PES		
	Absorption[b]	Calculation[c] (this work)	He 1[d]	This work	Calculation[c] (this work)
$\nu_1''(\nu_1^+)$	2782.5	2790	2580.2	⋯	2665
$\nu_2''(\nu_2^+)$	1746.1	1756	1674.8	⋯	1661
$\nu_3''(\nu_3^+)$	1500.6	1482	1210.2	1153	1206
$\nu_4''(\nu_4^+)$	1167.3	1165	771.1[e]	919	1037
$\nu_5''(\nu_5^+)$	2843.4	2846	⋯	2718	2744
$\nu_6''(\nu_6^+)$	1251.2	1221	⋯	814	818

[a]All values are in cm^{-1}.
[b]Data from Ref. 70.
[c]Calculated at B3LYP/6-311++G**, scaled by a factor of 0.9683.
[d]Data from Refs. 33 and 34.
[e]The present study supports the ν_6^+ (CH_2 rock) mode for this frequency.

TABLE II. Transition energies and vibrational frequencies of H_2CO [$^1A_2(3p_x)$, $^1A_1(3p_y)$, and $^1B_2(3p_z)$].[a]

	$^1A_2(3p_x)$		$^1A_1(3p_y)$		$^1B_2(3p_z)$	
	This work	Optical data[b]	This work	Optical data[c]	This work	Optical data[d]
Origin transition	67 730	67 779	64 262	64 251	65 483	65 451
ν_1'	⋯	⋯	⋯	⋯	⋯	2021
ν_2'	1791	⋯	⋯	⋯	1568	1679
ν_3'	1186	⋯	⋯	⋯	1334	1319
ν_4'	979	⋯	262[e]	307[e]	⋯	⋯
ν_5'	2696	2628	⋯	⋯	⋯	⋯
ν_6'	812	780	$1488(6_0^3)$	$1495(6_0^3)$	⋯	⋯

[a]All values are in cm^{-1}.
[b]Data from Ref. 21.
[c]Data from Ref. 19.
[d]Data from Ref. 23.
[e]The value corresponds to the lower inversion split component associated with the ν_4' level in the $^1A_1(3p_y)$ state.

calibration peaks, spanning the kinetic energy range from 1.45 to 1.85 eV—near the energy of the PES peak for H_2CO^+ in its vibrationless state. The peaks were least-squares fit by an empirical expression [Eq. (1)] to determine the calibration parameters t_0 and E_0,

$$\mathrm{KE} = \frac{m_e}{2}\left(\frac{L}{t-t_0}\right)^2 + E_0, \tag{1}$$

where KE is the kinetic energy of photoelectron, L is the length of flight path, t is the measured time of arrival, t_0 is an adjustable parameter representing the actual time of the ionization event, m_e is the mass of the electron, and E_0 is a parameter accounting for stray fields along the flight path. The absolute accuracy of Eq. (1) is ± 6 meV for the KE range covered by the Fe^+ calibration peaks (1.45–1.85 eV), and the relative uncertainty is ± 1.5 meV. Note, however, that for the high KE electrons generated when pumping the high vibrational levels of the $3p_x$ state, the uncertainty is higher and not known. This calibrated TOF-energy conversion expression was then used to assign all PES peaks for H_2CO^+.

III. RESULTS AND DISCUSSIONS

The neutral ground state of H_2CO $[\tilde{X}\,^1A_1]$ is planar with the dominant electronic configuration $(1a_1)^2\,(2a_1)^2(3a_1)^2\,(4a_1)^2(1b_2)^2\,(5a_1)^2(1b_1)^2(2b_2)^2$.[69] The vibrational fundamentals for ν_1'', ν_2'', ν_3'', ν_4'', ν_5'', and ν_6'' of H_2CO $[\tilde{X}\,^1A_1]$ are well known, and listed in Table I.[70] The excitation of a single electron from the oxygen nonbonding $2b_2$ orbital into a set of $3p_x$, $3p_y$, and $3p_z$ atomiclike orbitals leads to the Rydberg states $^1A_2(3p_x)$, $^1A_1(3p_y)$, and $^1B_2(3p_z)$, respectively, where the x axis is taken to be perpendicular to the molecular plane, the y axis is in the molecular plane, and z is the symmetry axis. Removal of an electron from the $2b_2$ orbital gives the $H_2CO^+[\tilde{X}\,^2B_2]$ state. We have also included, in Table I and Table II, the vibrational frequencies of H_2CO in the $^1A_2(3p_x)$, $^1A_1(3p_y)$, and $^1B_2(3p_z)$ intermediate states (ν') and in the cation ground state (ν^+), determined from ultraviolet absorption spectroscopy,[19,22,23] and He I photoelectron spectroscopy.[33,34] Here, ν_1'', ν_2'', ν_3'', ν_4'', ν_5'', and ν_6'' represent the CH_2 symmetric stretch (a_1), CO stretch (a_1), CH_2 scissors mode (a_1), CH_2 out-of-plane bend (b_1), CH_2 asymmetric stretch (b_2), and CH_2 rock (b_2), respectively.

A. The H_2CO [$^1A_1(3p_y)$ and $^1B_2(3p_z)$] states

In a C_{2v} molecule such as H_2CO, the transition from $2b_2$ to $3p$ orbitals is electric-dipole-allowed to the $3p_y$ and $3p_z$ orbitals, but forbidden to $3p_x$. For this reason, the $^1A_1(3p_y)$ and $^1B_2(3p_z)$ are well studied by single photon absorption,[16,18–25] yielding reliable transition energies for the formation of the vibrationless and vibronic levels of these two states. $3+1$ REMPI for the $^1A_1(3p_y)$ and $^1B_2(3p_z)$ state has also been reported,[29] however, the ion yields were small, and it was concluded that the high laser power required for REMPI led to line broadening and little spectroscopic information.

An *ab initio* study of the multiphoton properties of all three $3p$ Rydberg states has been reported by Galasso.[48] As he predicted, irrespective of the number of absorbed photons, the *np* Rydberg states have higher transition probabilities than the *nd* states, and the $^1A_1(3p_y)$ and $^1B_2(3p_z)$ states are more easily accessible than the $^1A_2(3p_x)$ state. Note, however, that because of the orbital symmetries, an electron in a $3p_y$ or $3p_z$ Rydberg orbital will tend to interact strongly with the valence orbitals lying in the molecular plane, while the $3p_x$ Rydberg orbital, perpendicular to the molecular plane, is less likely to be perturbed.

As shown in Fig. 2(a), the $2+1$ REMPI spectra of the $^1A_1(3p_y)$ and $^1B_2(3p_z)$ states are congested and poorly resolved, in contrast to that for the $^1A_2(3p_x)$ state (see below), which is sharp. In addition, the signal from REMPI via the $^1A_1(3p_y)$ and $^1B_2(3p_z)$ states is 15 times lower than that produced via $^1A_2(3p_x)$ excitation under similar conditions. Since we applied similar laser power in scanning all REMPI spectra, the broad peaks observed in Fig. 2(a) cannot be attributed to power broadening, as was suggested by Bomse and Dougal in discussion of their $3+1$ REMPI results.[29] The most reasonable explanation for the broadened and weak

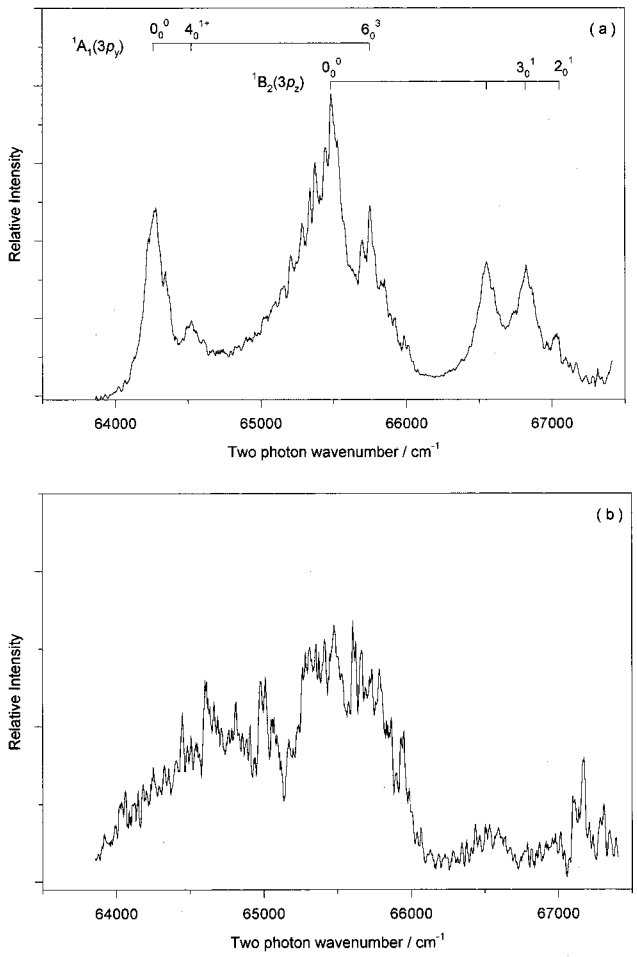

FIG. 2. (a) $2+1$ REMPI spectrum for $H_2CO[^1A_1(3p_y)$ and $^1B_2(3p_z)]$ obtained by measuring the total electron signal vs wavelength, (b) $2+1$ REMPI spectrum for $H_2CO[^1A_1(3p_y)$ and $^1B_2(3p_z)]$ obtained by measuring the H_2CO^+ signal vs wavelength.

spectra is that these two Rydberg states are strongly perturbed, resulting in reduced lifetime, and reduced ionization efficiency. Several types of perturbations are possible. The $^1A_1(3p_y)$ and $^1B_2(3p_z)$ states can interact with each other through the ν_6' mode. In addition, perturbation by the $^1A_1(\pi,\pi^*)[(a_1)^2(b_1)(b_2)^2(b_1^*)]$ and $^1B_1(\sigma,\pi^*)[(a_1)(b_1)^2(b_2)^2(b_1^*)]$ valence states is likely. Both of these valence configurations are embedded in the Rydberg energy region according to *ab initio* calculations, which place these states around 7.95 eV and 7.59 eV, respectively.[54] The $^1A_1(3p_y)$ state will interact with the $^1A_1(\pi,\pi^*)$ valence state. In addition, the $^1A_1(3p_y)$ state can vibronically couple to the $^1B_1(\sigma,\pi^*)$ valence state via the ν_4' mode, while the $^1B_2(3p_z)$ state can couple with the $^1A_1(\pi,\pi^*)$ valence state via the ν_5' and ν_6' modes. In contrast, the $^1A_2(3p_x)$ state is well separated from possible perturbing electronic states of the same symmetry. The only possible coupling is to the $^1B_1(\sigma,\pi^*)$ state, via the ν_5' and ν_6' modes, however, the coupling is expected to be weak because the energy difference between these two states is more than 0.8 eV.

The peak positions of the MPI bands resolved in Fig. 2(a) are listed in Table III. We have also included in Table III the positions of vibrational bands resolved in the single photon absorption work. The assignment for the MPI bands is achieved by comparison with the absorption data.[19,23] The origin band for $^1A_1(3p_y)$ is located at 64 262 cm^{-1}. This value is in good agreement with Price's value of 64 270 cm^{-1},[16] but blue shifted relative to Mentall *et al.*'s value of 64 251 cm^{-1},[19] and Lessard and Moule's value of 64 243 cm^{-1}.[23] In additional to the origin band, two vibrationally excited bands are resolved at 64 524 cm^{-1} and 65 750 cm^{-1}, respectively. The first excited band is also observed in single photon absorption and assigned to 4_0^{1+} by Mentall *et al.*,[19] the lower level of the inversion doublet that results from the out-of-plane distortion of this state. The inversion doubling is only resolvable in bands associated with ν_4', the out-of-plane bend. We use ''+'' and ''−'' to indicate the lower and upper levels of the corresponding inversion doublets. According to the absorption data, the upper level, 4_0^{1-}, of this inversion doublet is around 64 984 cm^{-1} with an inversion splitting of 460 cm^{-1},[19] however, this band was obscured by the broad origin band of the $^1B_2(3p_z)$ state, and cannot be identified. Note, that such assignment would require that the molecule be nonplanar in this intermediate, but with a small barrier to inversion. Just such inversion splitting was observed associated with the ν_4' excitation in the nonplanar $\tilde{A}\,^1A_2$ state of formaldehyde, and a fairly complete interpretation of the vibration structures associated with the ν_4' excitation in that state has been given by Walsh[71] and Brand.[14] Note, however, that the $3py$ Rydberg state is predicted to be planar according to *ab initio* calculations,[54] and the assignment associated with the ν_4' inversion splitting in the $3p_y$ state should be treated as tentative. The other excited band at 65 750 cm^{-1} is assigned as 6_0^3 following Lessard and Moule,[23] in which they reported a frequency of 444 cm^{-1} for ν_6'. Such an anomalously low ν_6' frequency might be the result of vibronic mixing between the $^1A_1(3p_y)$ and $^1B_2(3p_z)$ states, and/or between $^1A_1(3p_y)$ and the valence state $^1B_2(n,\sigma^*)[(a_1)^2(b_1)^2(b_2)(a_1^*)]$.

The $^1B_2(3p_z)$ origin is located at 65 483 cm^{-1}. This value is 35 cm^{-1} lower than Mentall's value of 65 518 cm^{-1},[19] and 32 cm^{-1} higher than Lessard and Moule's value of 65 451 cm^{-1}.[23] Three vibrational excited bands are re-

TABLE III. The two-photon resonant absorption positions, transition energies, and vibrational assignments for $H_2CO[^1A_1(3p_y)$ and $^1B_2(3p_z)]$.

Laser λ (nm)	Energy $2\nu_{vac}$ (cm^{-1})	ΔE[a] (cm^{-1})	Optical data[b] (cm^{-1})	Assignment
			$^1A_1(3p_y)$	
311.227	64 262	0	0	0_0^0
309.964	64 524	262	307	4_0^{1+c}
304.182	65 750	1488	1495	6_0^3
			$^1B_2(3p_z)$	
305.423	65 483	0	0	0_0^0
300.519	66 552	1069	1070	
299.325	66 817	1334	1319	3_0^1
298.281	67 051	1568	1679	2_0^1

[a]ΔE are energies measured with respect to $H_2CO[0_0^0,^1A_1(3p_y)]$ and $[0_0^0,^1B_2(3p_z)]$, respectively.
[b]Data from Refs. 19 and 23.
[c]The symbol ''+'' indicates the lower component of the inversion doublet.

solved at 66 552, 66 817, and 67 051 cm^{-1}, respectively, the last two of which are assigned to 3_0^1 and 2_0^1. This assignment yields frequencies for ν_3' and ν_2' of 1334 and 1568 cm^{-1}, respectively. The band at 66 552 cm^{-1} was also resolved in single photon absorption,[19] but its assignment is unclear. Both the positions and assignments of the vibrational bands is somewhat uncertain because of the broad and poorly resolved spectra. With exception of the ν_2' mode for $^1B_2(3p_z)$, the vibrational assignments for the $^1A_1(3p_y)$ and $^1B_2(3p_z)$ states determined from our MPI spectra are in good agreement with those from absorption measurements.

It is interesting to compare the REMPI spectrum taken by recording total electron yield [i.e., total ionization signal, Fig. 2(a)] with that recording only parent ion signal, Fig. 2(b). While the total electron yield spectrum is broad, there are still clearly resolvable spectral bands. In contrast, when monitoring parent ion production, the signal intensity is much lower. Most of the spectroscopic features disappear, leaving only a broad band near the origin position of the $^1B_2(3p_z)$ state with poor signal to noise ratio. The broad and weak total electron yield spectrum (compare to the $3p_x$ spectrum below) indicates that the $3p_y$ and $3p_z$ intermediate states undergo some radiationless process that reduces both their lifetimes and the ionization probability. The even lower intensity of the parent ion yield spectrum indicates that a large fraction of the nascent H_2CO^+ generated by REMPI absorb an additional photon and fragment. Fragmentation is discussed further below. The apparent increased width of the transitions in the parent ion spectrum, compared to the electron yield spectrum is probably not significant, but rather indicates that the REMPI signal has largely vanished into the non-resonant background. Anyway, neither state is at all useful for ion state-selection purpose.

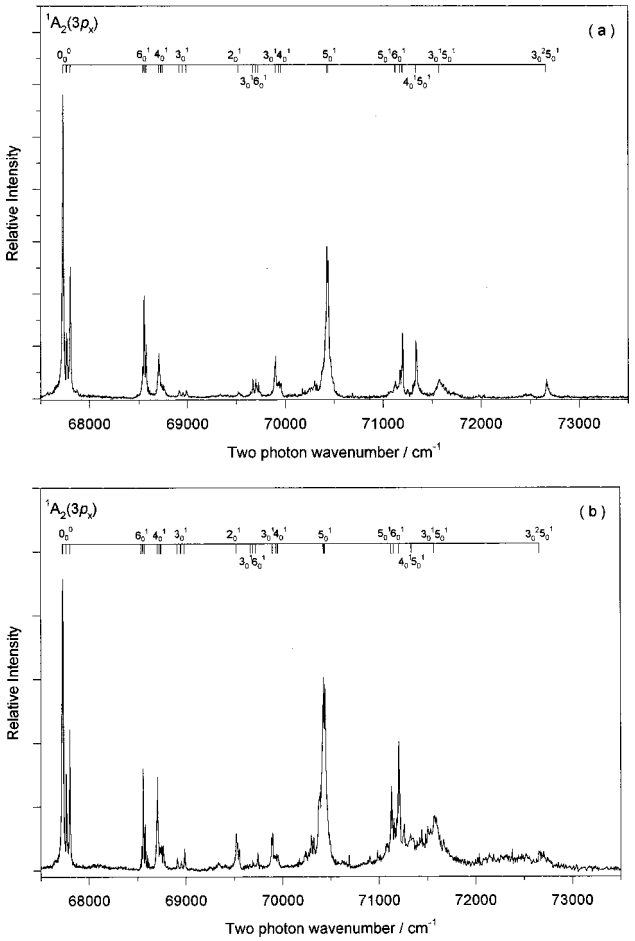

FIG. 3. (a) 2+1 REMPI spectrum for $H_2CO[^1A_2(3p_x)]$ obtained by measuring the total electron signal vs wavelength, (b) 2+1 REMPI spectrum for $H_2CO[^1A_2(3p_x)]$ obtained by measuring the H_2CO^+ signal vs wavelength.

B. The $H_2CO[^1A_2(3p_x)]$ state

1. 2+1 REMPI spectrum

As noted already, the $^1A_2(3p_x) \leftarrow \tilde{X}\,^1A_1$ origin transition was not observed in single photon spectroscopy, because it is electric dipole forbidden. The transition energy determined from other experiments is not in good agreement. Lessard and Moule estimated the origin to be at 67 779 cm^{-1} from absorption measurement of vibrational bands in the $^1A_2(3p_x)$ state.[21,23] The electron impact experiment of Taylor *et al.* suggested that this transition is electronic-quadrupole in nature and put the origin at 67 540 cm^{-1}.[28] More recently, Sun *et al.* estimated the origin to be 67 800 cm^{-1} from vibrational bands in 1+2+1 double resonance spectroscopy.[30] In addition, a number of calculations have been made to predict the $3p_x$ origin energy, with values of 9.07 eV (73 154 cm^{-1}) obtained using configuration interaction (CI)-PCMO by Peyerimhoff *et al.*,[40] 8.32 eV (67 105 cm^{-1}) obtained with a generalized valence bond (GVB)-CI calculation by Harding and Goddard,[43] 8.53 eV (68 799 cm^{-1}) obtained via random-phase-approximation by Galasso,[48] and 8.15 eV (65 734 cm^{-1}) obtained using multireference-CI by Hachey *et al.*[51,54]

Figure 3(a) shows the 2+1 REMPI spectrum in the vicinity of the $^1A_2(3p_x)$ state, at two-photon energies from 67 500 to 73 500 cm^{-1}. The assignments of the bands are indicated in the figure, and summarized in Table IV. As expected for two-photon selection rules, the origin of the $^1A_2(3p_x)$ state is clearly resolved in the 67 730–67 802 cm^{-1} region. The assignment of the origin band is based on comparison with the previous experimental data and its large intensity in the spectrum. The transition energy for the origin band (67 730 cm^{-1}) obtained here is 49–70 cm^{-1} lower than the values inferred from excited vibronic band positions in previous absorption and MPI experiments, and 190 cm^{-1} higher than the electron impact value. Because the origin band is strong and sharp in our spectrum, and our laser is calibrated to within ~2 cm^{-1} by fitting the rotationally resolved REMPI spectrum of NO, and the sharp Fe transitions used for PES calibration, we believe our value to be correct.

The origin band resolved in our REMPI spectrum is composed of three peaks, equally spaced by 36 cm^{-1}, and with roughly a 4:1:2 intensity ratio. Two possible assignments may account for this band contour. The first, suggested by Mentall *et al.* for the doublet origin band of the $^1A_1(3p_y)$ state,[19] is a pair of transitions terminating on the 0^+ and 0^- vibronic levels of an inversion manifold in the ν_4' mode. This assignment would require a nonplanar geometry for the $3p_x$ intermediate, and still leaves one of three peaks unexplained. The correct assignment for the triplet is as *K*

TABLE IV. The band positions, transition energies, and vibrational assignments for $H_2CO[^1A_2(3p_x)]$.

Laser λ (nm)	Energy $2\nu_{vac}$ (cm^{-1})	ΔE^a (cm^{-1})	Assignment
295.293	67 730	0	$0_0^0(R1)$
295.135	67 766	36	$0_0^0(R2)$
294.977	67 802	72	$0_0^0(R3)$
291.792	68 542	812	$6_0^1(R1)$
291.719	68 559	829	$6_0^1(R2)$
291.630	68 580	850	$6_0^1(R3)$
291.083	68 709	979	$4_0^1(R1)$
290.998	68 729	999	$4_0^1(R2)$
290.922	68 747	1017	$4_0^1(R3)$
290.207	68 916	1186	$3_0^1(R1)$
290.054	68 953	1223	$3_0^1(R2)$
289.910	68 987	1257	$3_0^1(R3)$
287.685	69 521	1791	2_0^1
287.063	69 671	1941	$3_0^1 6_0^1(R1)$
286.950	69 699	1969	$3_0^1 6_0^1(R2)$
286.848	69 723	1993	$3_0^1 6_0^1(R3)$
286.127	69 899	2169	$3_0^1 4_0^1(R1)$
285.988	69 933	2203	$3_0^1 4_0^1(R2)$
285.910	69 952	2222	$3_0^1 4_0^1(R3)$
283.986	70 426	2696	$5_0^1(R1)$
283.928	70 440	2710	$5_0^1(R2)$
281.197	71 125	3395	$5_0^1 6_0^1(R1)$
281.010	71 172	3442	$5_0^1 6_0^1(R2)$
280.909	71 197	3467	$5_0^1 6_0^1(R3)$
280.359	71 337	3607	$4_0^1 5_0^1(R1)$
280.332	71 344	3614	$4_0^1 5_0^1(R2)$
279.440	71 572	3842	$3_0^1 5_0^1/0_0^0, {}^1B_2(3d)$
275.245	72 663	4933	$3_0^2 5_0^1$

[a]ΔE are energies measured with respect to $H_2CO[0_0^0(R1), {}^1A_2(3p_x)]$.

rotational structure. The three components are, in order of increasing energy, the $\Delta K=0$, $K'=1\leftarrow K''=1$, $\Delta K=2$, $K'=2\leftarrow K''=0$, and $\Delta K=2$ $K'=3\leftarrow K''=1$ rotational branches (labeled below as $R1$,$R2$,$R3$). The three branches are spaced by 36 cm^{-1}, which is roughly equal to four times the A rotational constant.[70] With this assignment, the A constant is around 9 cm^{-1}—close to its value in the formaldehyde ground state. The alternation of intensities for $R1$, $R2$, and $R3$ is largely due to the 3:1 population of ortho and para modifications of H_2CO. The absence of any higher energy rotational lines indicates that only $K''=0$ and 1 states are significantly populated in our supersonically cooled formaldehyde beam.

The next intense MPI band located at 68 542–68 580 cm^{-1}, with partial resolved rotational structure, is assigned to the 6_0^1 transition. The prominent rotational band at 68 559 cm^{-1} was also observed in the single photon absorption spectrum of Lessard and Moule,[21,23] because this transition is weakly allowed by borrowing intensity from the intersecting $^1B_1$ valence state via vibronic coupling through the nontotally symmetric $\nu_6'(b_2)$ excitation. In that case, the vibronic symmetry of $^1A_2(3p_x)$ is $B_1^{e\nu}=A_2^e$ (electronic symmetry) $\times B_2^\nu$ (vibration symmetry). The frequency of ν_6' is determined to be 812 cm^{-1} from the present MPI measurement. This value is close to the ν_6^+ level in the cation (771.1 cm^{-1}) determined from He I PES.[33,34] We note that this 771.1 cm^{-1} frequency in the He I spectra was originally assigned as ν_4^+, but that our results support the reassignment to ν_6^+, originally suggested by Bruna *et al.*[57] (see below).

The MPI band at 68 709–68 747 cm^{-1} was not observed in single photon absorption, and the high intensity precludes assignment as a hot band. The vibrational frequency associated with this band is 979 cm^{-1}. We expect, as already shown for the ν_6 mode, that the frequencies of $H_2CO[^1A_2(3p_x)]$ should be similar to those of $H_2CO^+[\tilde{X}\,^2B_2]$ because the $3p_x$ state appears to be a well-behaved Rydberg state. From comparison with the cation frequencies given in Table I, this band is assigned to the ν_4' (out-of-plane bending) vibrational mode.

The set of small peaks around 68 916–68 987 cm^{-1} is readily assigned to the 3_0^1 transition. Since the ν_3' mode is totally symmetric (a_1), the rotational structure of this band is similar to that of the origin band. The $R1$, $R2$, and $R3$ rotational branches are centered at 68 916, 68 953, and 68 987 cm^{-1}, and the intensity alternations and line spacings are nearly identical to those of the origin band. The frequency of ν_3' is determined to be 1186 cm^{-1}. Again, we note the value of ν_3' is close to the value of ν_3^+ (1210.2 cm^{-1}) for the cation, determined from the He I PES measurement.[33,34] The weak peak at 69 521 cm^{-1} is assigned to the $2_0^1, {}^1A_2(3p_x)$ transition, resulting in a ν_2' frequency of 1791 cm^{-1}. The assignment is based on the similarity to the ν_2^+ frequency observed in He I photoelectron spectroscopy (1674.8 cm^{-1}),[33,34] and should be treated as tentative.

The next major bands at 69 671 cm^{-1} and 69 899 cm^{-1} are assigned to the combination bands $3_0^1 6_0^1$ and $3_0^1 4_0^1$, respectively. Since the ν_3' mode is totally symmetric, the $3_0^1 6_0^1$ and $3_0^1 4_0^1$ bands show similar rotational profiles to those of the 6_0^1 and 4_0^1 bands, respectively. For all of these vibrational components, the rotational line spacings are substantially reduced (~19 cm^{-1} in 6_0^1 and 4_0^1 and ~26 cm^{-1} in $3_0^1 6_0^1$ and $3_0^1 4_0^1$), compared to those observed for the origin and 3_0^1 bands, which implies a reduction in the A constant, as expected for vibronic levels with ν_4' CH_2 out-of-plane bend and ν_6' CH_2 rock excitation.

Excitation of the ν_5' mode (b_2) has been observed in single photon absorption, because it also is allowed by vibronic coupling. In that absorption work, the 5_0^1 transition was assigned at 70 407±20 cm^{-1},[21] and we have, accordingly, assigned our partially resolved band peaking at 70 426 cm^{-1} and 70 440 cm^{-1} to the 5_0^1 transition. The frequency of ν_5' determined in the present MPI spectrum is 2696 cm^{-1}. We note that both ν_5' and ν_6' reported in the absorption study (2628 cm^{-1} and 780 cm^{-1}) are in error by more than 20 cm^{-1} uncertainty in the 5_0^1 and 6_0^1 band positions.[21] The discrepancy is attributable to the fact that their estimated position for the (forbidden) origin band was 49 cm^{-1} higher than our directly measured value.

We also observe combination bands attributed to the $5_0^1 6_0^1$ and $4_0^1 5_0^1$, at 71 125–71 197 cm^{-1} and 71 337–71 344 cm^{-1}, respectively. Due to the vibronic symmetry changes when combined with the nontotally symmetric $\nu_5'(b_2)$ mode, the rotational contours of the $5_0^1 6_0^1$ and $4_0^1 5_0^1$ bands are quite different from those of the $6_0^1(3_0^1 6_0^1)$ and $4_0^1(3_0^1 4_0^1)$ bands, respectively.

In the energy region above 71 500 cm^{-1}, the vibrational

bands of the $^1A_2(3p_x)$ state begin to overlap with those of the $^1B_2(3d)$ state. Without the photoelectron spectral data (below), the broad band at 71 572 cm^{-1} would have been a good candidate for the origin band of the $^1B_2(3d)$ state, and the peak at 72 663 cm^{-1} might be assigned as 3_0^1 of the $^1B_2(3d)$ state.[23] The photoelectron spectra indicate that these two bands are actually transitions to high vibrational levels of the $^1A_2(3p_x)$ state, although the former is strongly perturbed by interaction with the $3d$ state origin. These peaks are assigned as the $3_0^1 5_0^1$ and $3_0^2 5_0^1$ transitions to the $^1A_2(3p_x)$ state, respectively.

We also recorded the $^1A_2(3p_x)$ REMPI spectrum, measuring the parent ion signal vs wavelength, as shown in Fig. 3(b). Generally, the parent ion yield and total electron yield spectra are quite similar. No evidence is found for a nonresonant background, and almost all the vibronic bands observed for parent ions are consistent with those observed with electrons. There are some significant intensity differences, however. Note that in Fig. 3(a), the intensity of the peak for 2_0^1 at 69 521 cm^{-1} is very weak, while in Fig. 3(b), this band has substantial intensity. In contrast, the relative intensity of peaks in the total electron yield spectrum [Fig. 3(a)] at 69 699 $cm^{-1}(3_0^1 6_0^1, R2)$, 71 337/71 344 $cm^{-1}(4_0^1 5_0^1, R1, R2)$, and 72 663 $cm^{-1}(3_0^2 5_0^1)$ decrease substantially when the parent ion yield is monitored. The most likely explanation is that the cations produced via these resonances have a particularly high probability of absorbing additional photons, and fragmenting. This decreases their contribution to the parent ion yield spectrum, but not to the total electron yield spectrum. For the 2_0^1 band, which increases in relative intensity in the parent ion spectrum, the converse is presumably true. Cations produced via this resonance are less likely than average to absorb additional photons and fragment. Because the relative collection/detection efficiencies for electrons and cations are unknown, and probably different, it is not possible to directly compare the signal levels in the electron and parent ion yield spectra. It is clear from the REMPI mass spectra (below), however, that a substantial fraction of the nascent ions fragment. As a consequence, changes in the fragmentation probability can strongly affect the relative peak intensities in the parent ion yield spectrum.

2. MPI time-of-flight photoelectron spectra

Photoelectron spectra (PES) were taken pumping through all the major bands in the $^1A_2(3p_x)$ state. The ion internal energy (E_{int}) associated with each photoelectron band is calculated from the position of the band center by Eq. (2),

$$E_{int} = (2+1)h\nu - \mathrm{KE} - \mathrm{IP}, \tag{2}$$

where KE is the measured photoelectron kinetic energy, and IP is 10.88 eV according to the NIST chemistry WebBook.[72] The PES in Fig. 4 have been transformed to an ion internal energy scale for ease of comparison, and a summary of the measured ion internal energies is given in Table V. As shown in Fig. 4, with one exception, each photoelectron spectrum has a single significant peak, indicating that for all $3p_x$ REMPI transitions, cations are produced in a single vibrational state. Indeed, the ion internal energies are very close to the energies of the vibrations pumped in the $3p_x$ intermediate state, suggesting that the ionization Franck–Condon factors are diagonal, i.e., there is a propensity to preserve the vibration selected at the intermediate level. For the relatively high KE electrons produced in $2+1$ REMPI through this state, the photoelectron energy resolution is 40 meV ($\sim$320 cm^{-1}), as estimated from the full width at half maximum (FWHM) of the Fe^+ photoelectron peaks, which

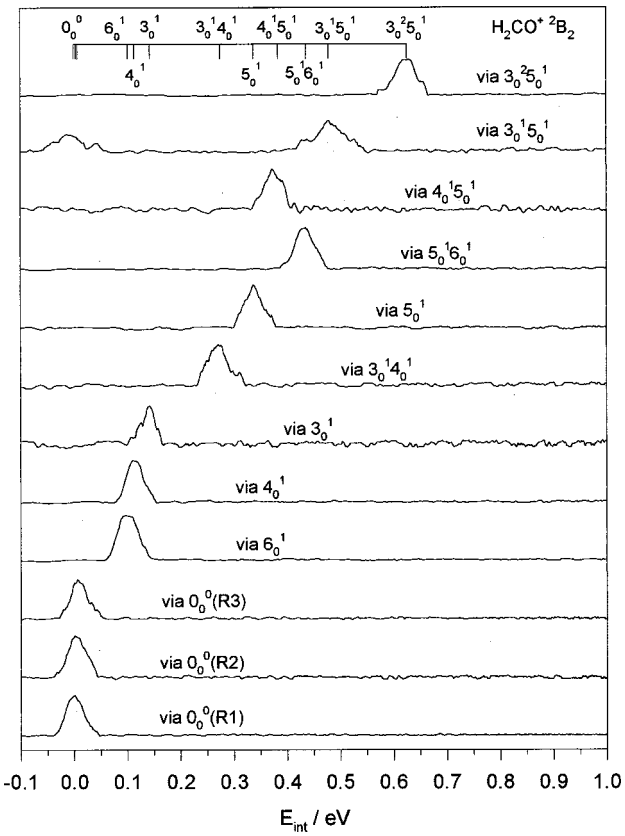

FIG. 4. Photoelectron spectra taken following REMPI via various vibronic levels of $H_2CO[^1A_2(3p_x)]$.

TABLE V. Multiphoton ionization PES of $H_2CO^+[\tilde{X}\,^2B_2]$ via $H_2CO[^1A_2(3p_x)]$.

Laser λ (nm)	Intermediate state $H_2CO[^1A_2(3p_x)]$	E_{int} (meV)	$\Delta\nu^b$ (cm^{-1})	Ionic state $H_2CO^+[\tilde{X}\,^2B_2]$
295.293	$0_0^0(R1)$	0	0	0_0^0
295.135	$0_0^0(R2)$	4	32	0_0^0
294.977	$0_0^0(R3)$	7	56	0_0^0
291.719	6_0^1	101	814	6_0^1
291.083	4_0^1	114	919	4_0^1
290.207	3_0^1	143	1153	3_0^1
286.133	$3_0^1 4_0^1$	275	2218	$3_0^1 4_0^1$
283.986	5_0^1	337	2718	5_0^1
280.909	$5_0^1 6_0^1$	436	3516	$5_0^1 6_0^1$
280.359	$4_0^1 5_0^1$	384	3097	$4_0^1 5_0^1$
279.440	$3_0^1 5_0^1/[0_0^0, {}^1B_2(3d)]$	479/−2[a]	3863/0	$3_0^1 5_0^1/0_0^0$
275.245	$3_0^2 5_0^1$	626	5049	$3_0^2 5_0^1$

[a]Negative 2 meV is within the experimental uncertainty, and thus is treated as 0 meV.

[b]$\Delta\nu$ are vibrational energies measured with respect to the PES band obtained when pumping through $H_2CO[0_0^0(R1), {}^1A_2(3p_x)]$.

have similar KEs. The measured formaldehyde PES peak widths are 35–50 meV (FWHM). The uncertainty in the vibrational frequencies deduced, depends only on the relative energies of the bands, and is limited by the uncertainty in determining band centers, and possible non-linearities in the energy scale. The uncertainty is estimated to be less than ± 3 meV or ± 24 cm^{-1}.

To aid assignment of the ion vibrations, *ab initio* calculations were performed with MP2, B3LYP theories using GAUSSIAN 98,[73] in both cases using the 6-311++G** basis set. As a check on the calculated cation frequencies, we also calculated the vibrational frequencies of neutral formaldehyde, where a complete set of experimental frequencies is available. It turns out that the B3LYP/6-311++G** results are in best overall agreement, and these have been used in the analysis. As is often the case, the *ab initio* frequencies are systematically higher than the neutral ground state frequencies. This systematic error has been corrected by scaling the *ab initio* frequencies by a factor of 0.9683 for neutral. The same scale factor was then used to scale the cation *ab initio* frequencies for comparison with our experimental results. The scaled *ab initio* and experimental frequencies are compared in Table I. Given the diagonal nature of the ionization transitions and the excellent agreement with the *ab initio* frequencies, assignment of the photoelectron spectra is straightforward.

The first three PES result from ionization through the $R1$, $R2$, and $R3$ rotational branches of the vibrationless level of $^1A_2(3p_x)$. Unambiguously, the peaks in these photoelectron spectra correspond to the formation of H_2CO^+ in the vibrationless ground state, and the ion internal energy difference of $\sim$3.5 meV (30 cm^{-1}) between these peaks indicates a propensity to preserve the K rotational state in ionization. Recent studies of rotationally resolved photoelectron spectra revealed that the rotational spacing of $H_2CO^+[0_1^0,\tilde{X}\,^2B_2]$ is also mainly determined by the A rotational constant (8.875 cm^{-1}).[36]

The ion internal energy for the PES obtained via the $6_0^1,{}^1A_2(3p_x)$ transition is 814 cm^{-1}. Based on the good agreement with the calculated value of the ν_6^+ frequency (818 cm^{-1}) and the propensity for diagonal ionization, this PES band is assigned to the ν_6^+ mode. Note, that a band was observed in the He I PES (Refs. 33, 34) with a frequency of 771.1 cm^{-1}, and assigned as ν_4^+. Obviously, there would be large discrepancy between experimental and calculated frequency value if this assignment was true. Furthermore, the observation of the ν_4^+ fundamental in the He I PES, would require a nonplanar cation structure, because odd quanta of such symmetry-breaking vibrations is normally not allowed in PES if both neutral and cation ground states are planar.[33,34] On the other hand, calculations at the B3LYP, MP2, CASSCF, and CCSD(T) levels, with various basis sets including cc-pVDZ and 6-311++G**, all converge to a planar cation geometry, and planar geometry was also found in earlier theoretical work.[54,56,57] We, therefore, concur with the reassignment of this band to the ν_6^+ mode, as suggested by Bruna *et al.*[57]

The PES pumped through the $4_0^1,{}^1A_2(3p_x)$ transition is assigned to the excitation of ν_4^+ in the cation, based on the propensity for diagonal ionization. This assignment results in a frequency for ν_4^+ of 919 cm^{-1}. Note, that this experimental frequency is 118 cm^{-1} lower than the calculated ν_4^+ frequency (Table I), which is well outside the experimental uncertainty. Note that a calculation at the QCISD/cc-pVTZ level yielded 1055 cm^{-1} for the ν_4^+ frequency,[56] in good agreement with our calculated result. As there is no good alternative to the ν_4^+ assignment, we conclude that the ν_4^+ mode must be unusually anharmonic. Note that the appearance of strong bands associated with the out-of-plane bend in both the REMPI and PES spectra, implies that some state involved in the 2+1 REMPI process is bent. The neutral ground state is clearly planar, and the cation ground state also is calculated to be planar, with some confidence. We conclude that the $^1A_2(3p_x)$ intermediate must be bent, allowing ν_4 Franck–Condon activity in both the two-photon excitation, and ionization steps.

The PES band obtained following REMPI through the $3_0^1,{}^1A_2(3p_x)$ transition is readily assigned to ν_3^+ of H_2CO^+. The frequency of ν_3^+ is around 1153 cm^{-1} in our measurement, and we note that there is 57 cm^{-1} difference between our value of ν_3^+ and that obtained from the He I measurement. The deviation results partly from the combined uncertainty in the two experiments, but also is affected by the unresolved rotational structure in both REMPI and He I PES. In our experiment, the PES was obtained by pumping the $\Delta K=0$, $K'=1\leftarrow K''=1(R1)$ rotational transition, so that range of K in the cation is restricted, while in the He I PES the entire neutral ground state K manifold is ionized.

No good PES measurements were obtained pumping through the 2_0^1 and $3_0^1 6_0^1,{}^1A_2(3p_x)$ transitions, because these transitions are too weak. The cation vibrational energy associated with the PES peak resulting from ionization through the $3_0^1 4_0^1,{}^1A_2(3p_x)$ transition is 2218 cm^{-1}—a reasonable match to the expected combination frequency, taking into account the large anharmonicity of ν_4^+.

Excitation of the ν_5^+ mode in the cation results from REMPI through the $5_0^1,{}^1A_2(3p_x)$ transition. Because this mode is not totally symmetric, it has not been reported in previous PES experiments. The frequency of ν_5^+ is measured to be 2718 cm^{-1}, which is in good agreement with the calculated value of 2744 cm^{-1}. REMPI through the $5_0^1 6_0^1,{}^1A_2(3p_x)$ transition results in cations with $\nu_5^+\nu_6^+$ combination excitation. The combination frequency (3516 cm^{-1}) is within a few wave numbers of the sum of ν_5^+ and ν_6^+ frequencies, indicating that this combination is quite harmonic. The PES peak obtained following ionization through the $4_0^1 5_0^1,{}^1A_2(3p_x)$ transition is assigned to the $\nu_4^+\nu_5^+$ combination excitation, again based on the strong propensity for diagonal ionization. Note, however, that the resulting combination frequency (3097 cm^{-1}) is 540 cm^{-1} lower than the sum of ν_4^+ and ν_5^+ frequencies. The accuracy of the extracted ion vibrational energies is reduced for these high energy excitations, because the associated photoelectron kinetic energies are beyond the calibration energy range. Nonetheless, we estimate that the error should still be within 80 cm^{-1}. The simplest rationalization for the large frequency discrepancy is to invoke strong anharmonicity, and we note that the PES band associated with the ν_4^+ fundamental is also shifted to

lower energy relative to the calculated, harmonic frequency.

The PES following ionization of $H_2CO[3_0^1 5_0^1, {}^1A_2(3p_x)]$ is the only one which shows two peaks. Within the experimental uncertainty, the peak at low internal energy corresponds to production of cations in the ground vibrational state. The slow electron (i.e., high ion internal energy) peak corresponds to an ion vibrational energy of 3863 cm^{-1}, and we assign this to the cation $\nu_3^+ \nu_5^+$ combination band. This assignment, in turn, leads us (see above) to assign the REMPI band at 71 572 cm^{-1} as a mixed state with contributions from both $H_2CO[0_0^0, {}^1B_2(3d)]$ and $H_2CO[3_0^1 5_0^1, {}^1A_2(3p_x)]$. The mixed nature of this intermediate vibronic level presumably also accounts for its broadening in the REMPI spectrum, Fig. 3(a). The final PES is for cations produced via the $3_0^2 5_0^1, {}^1A_2(3p_x)$ transition. The peak observed corresponds to an ion vibrational energy of 5049 cm^{-1}, in good agreement with the energy expected for the $2\nu_3^+ + \nu_5^+$ combination in the cation.

From our perspective of looking for cation mode-selective ionization routes, the formaldehyde $^1A_2(3p_x)$ state is nearly ideal. The Franck–Condon factors for ionization are nearly perfectly diagonal, indicating that there is little geometry change between the $3p_x$ and cation states, and that the $3p_x$ levels are not significantly perturbed (except for the $3_0^1 5_0^1$ band). This is a rare case where REMPI produces essentially perfectly state-selected ions, over a very wide range of ion internal energies, and with excitation of several types of vibrational motion possible. Given the shifts in PES band positions when pumping through different rotational lines of the origin band, it appears that it is even possible to select a limited range of cationic *K* states.

3. Ion photofragmentation

Photodissociation and dissociative ionization of the H_2CO molecule has been extensively studied experimentally and theoretically.[74–87] There are two low-energy dissociation channels for the cation, producing HCO^+ and CO^+ with appearance thresholds of 11.97 eV (Ref. 81) and 14.10 eV,[37] respectively. Relative to the cation ground state (IP = 10.88 eV), the dissociation channels are

$$H_2CO^+ \rightarrow HCO^+ + H \quad \Delta H = 1.09 \text{ eV}$$
$$\rightarrow CO^+ + H_2 \quad \Delta H = 3.22 \text{ eV}.$$

Both fragment channels are observed in the REMPI mass spectra taken via the $^1A_2(3p_x)$ intermediate state. Some trends are obvious on comparison of the mass spectra obtained via different vibronic levels of $^1A_2(3p_x)$. The intensities of H_2CO^+ and HCO^+ are always much higher than that of CO^+, and the ratio of H_2CO^+ to HCO^+ differs markedly for ionization via different intermediate vibronic levels. Generally, more HCO^+ appears in the mass spectra when pumping through higher vibronic levels, and high laser power yields a high degree of fragmentation. Figure 5 shows a typical mass spectrum taken at 286.127 nm via the $3_0^1 4_0^1, {}^1A_2(3p_x)$ intermediate.

Production of HCO^+ is energetically possible directly in the 2+1 REMPI process. Note, however, that such a dissociative ionization process is inconsistent with the observation

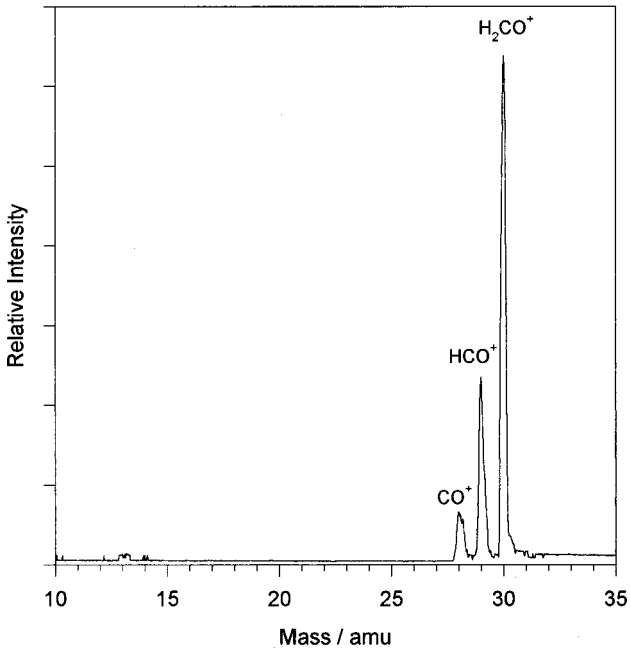

FIG. 5. Multiphoton ionization mass spectrum of H_2CO via the $H_2CO[3_0^1 4_0^1, {}^1A_2(3p_x)]$ resonant state at 286.127 nm.

of a single, sharp peak in the photoelectron spectra. The spectra clearly show that only parent ions are formed in the REMPI process, and that the vibrational excitation in the nascent ions is well below the dissociation limit. Fragmentation must, therefore, be attributable to photodissociation of the nascent H_2CO^+ parent cations,

$$H_2CO(\tilde{X}\,{}^1A_1) \overset{2+1}{\rightarrow} H_2CO^+(\tilde{X}\,{}^2B_2) + e^- \overset{1}{\rightarrow} HCO^+ + H + e^-.$$

The production of CO^+ presumably also involves photodissociation, in this case requiring an additional photon. The fact that cations which absorb an additional photon fragment, is actually very important in REMPI state selection, because it removes any cations that have been excited out of the desired vibrational level of the ground state.

ACKNOWLEDGMENTS

This work was supported by the National Science Foundation under Grant No. CHE-9807625. We are grateful to Professor Jack Simons, Professor Michael Morse, and Professor Alex Boldyrev (Utah State) for helpful discussions concerning the interpretation of this work.

[1] C. L. Liao, C. X. Liao, and C. Y. Ng, Chem. Phys. Lett. **103**, 418 (1984).
[2] C. L. Liao, R. Xu, and C. Y. Ng, J. Chem. Phys. **85**, 7136 (1986).
[3] C. L. Liao, R. Xu, G. D. Flesch, M. Baer, and C. Y. Ng, J. Chem. Phys. **93**, 4818 (1990).
[4] L. A. Posey, R. D. Guettler, N. J. Kirchner, and R. N. Zare, J. Chem. Phys. **101**, 3772 (1994).
[5] R. D. Guettler, G. C. Jones, Jr., L. A. Posey, and R. N. Zare, Science **266**, 259 (1994).
[6] Y.-H. Chiu, H. Fu, J.-T. Huang, and S. L. Anderson, J. Chem. Phys. **102**, 1199 (1995).
[7] Y.-H. Chiu, H. Fu, J.-T. Huang, and S. L. Anderson, J. Chem. Phys. **105**, 3089 (1996).
[8] S. L. Anderson, Acc. Chem. Res. **30**, 28 (1997).
[9] J. Qian, H. Fu, and S. L. Anderson, J. Phys. Chem. **101**, 6504 (1997).

[10] H. Fu, J. Qian, R. J. Green, and S. L. Anderson, J. Chem. Phys. **108**, 2395 (1998).
[11] J. Qian, R. J. Green, and S. L. Anderson, J. Chem. Phys. **108**, 7173 (1998).
[12] R. J. Green, H.-T. Kim, J. Qian, and S. L. Anderson, J. Chem. Phys. **113**, 4158 (2000).
[13] S. L. Anderson, Adv. Chem. Phys. **82**, 177 (1992).
[14] J. C. D. Brand, J. Chem. Soc. 858 (1956).
[15] H. H. Nielsen, Phys. Rev. **46**, 117 (1934).
[16] W. C. Price, J. Chem. Phys. **3**, 256 (1935).
[17] E. S. Ebers and H. H. Nielsen, J. Chem. Phys. **6**, 311 (1938).
[18] G. Fleming, M. M. Anderson, A. J. Harrison, and L. W. Pickett, J. Chem. Phys. **30**, 351 (1959).
[19] J. E. Mentall, E. P. Gentieu, M. Krauss, and D. Neumann, J. Chem. Phys. **55**, 5471 (1971).
[20] C. R. Lessard, D. C. Moule, and S. Bell, Chem. Phys. Lett. **29**, 603 (1974).
[21] C. R. Lessard and D. C. Moule, J. Mol. Spectrosc. **60**, 343 (1976).
[22] C. R. Drury-Lessard and D. C. Moule, Chem. Phys. Lett. **47**, 300 (1977).
[23] C. R. Lessard and D. C. Moule, J. Chem. Phys. **66**, 3908 (1977).
[24] P. Brint, J.-P. Connerade, C. Mayhew, and K. Sommer, J. Chem. Soc., Faraday Trans. 2 **81**, 1643 (1985).
[25] G. Cooper, J. E. Anderson, and C. E. Brion, Chem. Phys. **209**, 61 (1996).
[26] G. C. Causley and B. R. Russell, J. Am. Chem. Soc. **101**, 5573 (1979).
[27] E. H. VanVeen, W. L. VanDijk, and H. H. Brongersma, Chem. Phys. **16**, 337 (1976).
[28] S. Taylor, D. G. Wilden, and J. Comer, Chem. Phys. **70**, 291 (1982).
[29] D. S. Bomse and S. Dougal, Laser Chem. **7**, 35 (1987).
[30] W. Z. Sun, X. B. Xie, L. Li, and C. H. Zhang, Chin. J. Chem. Phys. **2**, 184 (1989).
[31] X. N. Li, X. B. Xie, L. Li, and C. H. Zhang, Chin. J. Chem. Phys. **4**, 235 (1991).
[32] A. D. Baker, C. Baker, C. R. Brundle, and D. W. Turner, Int. J. Mass Spectrosc. **1**, 285 (1968).
[33] B. Niu, D. A. Shirley, Y. Bai, and E. Daymo, Chem. Phys. Lett. **201**, 212 (1993).
[34] B. Niu, D. A. Shirley, and Y. Bai, J. Chem. Phys. **98**, 4377 (1993).
[35] D. M. P. Holland, M. A. Hayes, M. A. MacDonald, and S. M. McSweeney, J. Phys. B **27**, 1125 (1994).
[36] R. T. Wiedmann, M. G. White, K. Wang, and V. McKoy, J. Chem. Phys. **100**, 4738 (1994).
[37] P. M. Guyon, W. A. Chupka, and J. Berkowitz, J. Chem. Phys. **64**, 1419 (1976).
[38] S. V. Andreyev, V. S. Antonov, I. N. Knyazev, and V. S. Letokhov, Chem. Phys. Lett. **45**, 166 (1977).
[39] J. L. Whitten and M. Hackmeyer, J. Chem. Phys. **51**, 5584 (1969).
[40] S. D. Peyerimhoff, R. J. Buenker, W. E. Kammer, and H. Hsu, Chem. Phys. Lett. **8**, 129 (1971).
[41] T. C. Betts and V. McKoy, J. Chem. Phys. **60**, 2947 (1974).
[42] L. S. Cederbaum, W. Domcke, and W. VonNiessen, Chem. Phys. Lett. **34**, 60 (1975).
[43] L. B. Harding and W. A. Goddard, J. Am. Chem. Soc. **99**, 677 (1977).
[44] P. W. Langhoff, A. E. Orel, T. N. Rescigno, and B. V. McKoy, J. Chem. Phys. **69**, 4689 (1978).
[45] A. N. Singh and R. S. Prasad, Chem. Phys. **49**, 267 (1980).
[46] D. J. DeFrees and A. D. McLean, J. Chem. Phys. **82**, 333 (1985).
[47] W. D. Allen and H. F. Schaefer, J. Chem. Phys. **87**, 7076 (1987).
[48] V. Galasso, J. Chem. Phys. **92**, 2495 (1990).
[49] K. Takeshita, J. Chem. Phys. **94**, 7259 (1991).
[50] A. Cesar, H. Ågren, T. Helgaker, P. Jørgensen, and H. J. A. Jensen, J. Chem. Phys. **95**, 5906 (1991).
[51] M. R. J. Hachey, P. J. Bruna, and F. Grein, J. Phys. Chem. **99**, 8050 (1995).
[52] P. J. Bruna, M. R. J. Hachey, and F. Grein, J. Phys. Chem. **99**, 16576 (1995).
[53] M. Merchan and B. O. Roos, Theor. Chim. Acta **92**, 227 (1995).
[54] M. R. J. Hachey, P. J. Bruna, and F. Grein, J. Mol. Spectrosc. **176**, 375 (1996).
[55] L. Singleton and P. Brint, J. Chem. Soc., Faraday Trans. **93**, 11 (1997).
[56] S. C. Kuo, Z. Y. Zhang, S. K. Ross, R. B. Klemm, R. D. Johnson, P. S. Monks, R. P. Thorn, and L. J. Stief, J. Phys. Chem. A **101**, 4035 (1997).
[57] P. J. Bruna, M. R. J. Hachey, and F. Grein, Mol. Phys. **94**, 917 (1998).
[58] M. B. Robin, *Higher Excited States of Polyatomic Molecules* (Academic, New York, 1985).
[59] B. A. Heath, M. B. Robin, N. A. Kuebler, G. J. Fisanick, and T. S. Eichelberger, J. Chem. Phys. **72**, 5565 (1980).
[60] G. J. Fisanick, T. S. Eichelberger, B. A. Heath, and M. B. Robin, J. Chem. Phys. **72**, 5571 (1980).
[61] T. S. Eichelberger and G. J. Fisanick, J. Chem. Phys. **74**, 5962 (1981).
[62] H.-T. Kim and S. L. Anderson, J. Chem. Phys. **114**, 3018 (2001).
[63] R. Spence and W. Wild, J. Chem. Soc. 338 (1935).
[64] F. S. Dainton, K. J. Ivin, and D. A. G. Walmsley, Trans. Faraday Soc. **55**, 61 (1959).
[65] F. A. Baiocchi and W. Klemperer, J. Chem. Phys. **78**, 3509 (1983).
[66] S. L. Anderson, L. Goodman, K. Krogh-Jespersen, A. G. Ozkabak, R. N. Zare, and C.-F. Zheng, J. Chem. Phys. **82**, 5329 (1985).
[67] R. L. Whetten, K.-J. Fu, and E. R. Grant, J. Chem. Phys. **79**, 4899 (1983).
[68] J. Sugar and C. Corliss, J. Phys. Chem. Ref. Data **14** (Suppl. 2), 407 (1985).
[69] D. C. Moule and A. D. Walsh, Chem. Rev. **75**, 67 (1975).
[70] G. Herzberg, *Molecular Spectra and Molecular Structure III. Electronic Spectra and Electronic Structure of Polyatomic Molecules* (Van Nostrand Reinhold, New York, 1966).
[71] A. D. Walsh, J. Chem. Soc. 2306 (1953).
[72] S. G. Lias, J. E. Bartmess, J. F. Liebman, J. L. Holmes, R. D. Levin, and W. G. Mallard, in *NIST Chemistry Webbook, NIST Standard Reference Database Number 69*, edited by W. G. Mallard and P. J. Linstrom (National Institute of Standards and Technology, Gaithersburg, MD, 2000), http://webbook.nist.gov.
[73] M. J. Frisch, G. W. Tucks, H. B. Schlegel *et al.*, GAUSSIAN98 (Gaussian, Inc., Pittsburgh, PA, 1998).
[74] C. S. Matthews and P. Warneck, J. Chem. Phys. **51**, 854 (1969).
[75] M. Vaz Pires, C. Galloy, and J. C. Lorquet, J. Chem. Phys. **69**, 3242 (1978).
[76] R. Bombach, J. Dannacher, J.-P. Stadelmann, and J. Vogt, Int. J. Mass Spectrom. Ion Phys. **40**, 275 (1981).
[77] R. Bombach, J. Dannacher, J.-P. Stadelmann, and J. Vogt, Chem. Phys. Lett. **77**, 399 (1981).
[78] P. Ho, D. J. Bamford, R. J. Buss, Y. T. Lee, and C. B. Moore, J. Chem. Phys. **76**, 3630 (1982).
[79] C. Barbier, C. Galloy, and J. C. Lorquet, J. Chem. Phys. **81**, 2975 (1984).
[80] H. Wankenne, G. Caprace, and J. Momigny, Int. J. Mass Spectrom. Ion Processes **57**, 149 (1984).
[81] J. C. Traeger, Int. J. Mass Spectrom. Ion Processes **66**, 271 (1985).
[82] C. B. Moore and D. J. Bamford, Laser Chem. **6**, 93 (1986).
[83] H. X. Liu, Z. L. Li, S. T. Li, J. C. Han, and C. K. Wu, Acta Phys. Sin. (Overseas Ed.) **37**, 470 (1988).
[84] J. C. Lorquet and T. Takeuchi, J. Phys. Chem. **94**, 2279 (1990).
[85] A. C. Terentis, S. E. Waugh, G. F. Metha, and S. H. Kable, J. Chem. Phys. **108**, 3187 (1998).
[86] O. K. Abou-Zied and J. D. McDonald, J. Chem. Phys. **109**, 1293 (1998).
[87] L. R. Valachovic, M. F. Tuchler, M. Dulligan, T. Droz-Georget, M. Zyrianov, A. Kolessov, H. Reisler, and C. Wittig, J. Chem. Phys. **112**, 2752 (2000).